Pathways of Pacific water across the Chukchi Sea: A numerical model study

Peter Winsor and David C. Chapman

Physical Oceanography Department, Woods Hole Oceanographic Institution, Woods Hole, Massachusetts, USA

Received 16 May 2003; revised 29 September 2003; accepted 17 November 2003; published 2 March 2004.

[1] Pathways of Pacific Water flowing from the North Pacific Ocean through Bering Strait and across the Chukchi Sea are investigated using a two-dimensional barotropic model. In the no-wind case, the flow is driven only by a prescribed steady northward flow of 0.8 Sv through Bering Strait. The resulting steady state circulation consists of a broad northeasterly flow, basically following the topography, with a few areas of intensified currents. About half of the inflow travels northwest through Hope Valley, while the other half turns somewhat toward the northeast along the Alaskan coast. The flow through Hope Valley is intensified as it passes through Herald Canyon, but much of this flow escapes the canyon to move eastward, joining the flow in the broad valley between Herald and Hanna Shoals, another area of slightly intensified currents. There is a confluence of nearly all of the flow along the Alaskan coast west of Pt. Barrow to create a very strong and narrow coastal jet that follows the shelf topography eastward onto the Beaufort shelf. Thus in this no-wind case, nearly all of the Pacific Water entering the Chukchi Sea eventually ends up flowing eastward along the narrow Beaufort shelf, with no discernable flow across the shelf edge toward the interior Canada Basin. Travel times for water parcels to move from Bering Strait to Pt. Barrow vary tremendously according to the path taken; e.g., less than 6 months along the Alaskan coast, but about 30 months along the westernmost path through Herald Canyon. This flow field is relatively insensitive to idealized wind-forcing when the winds are from the south, west or north, in which cases the shelf transports tend to be intensified. However, strong northeasterly to easterly winds are able to completely reverse the flows along the Beaufort shelf and the Alaskan coast, and force most of the throughflow in a more northerly direction across the Chukchi Sea shelf edge, potentially supplying the surface waters of the interior Canada Basin with Pacific Water. The entire shelf circulation reacts promptly to changing wind conditions, with a response time of $\sim$2–3 days. The intense coastal jet between Icy Cape and Pt. Barrow implies that dense water formed here from winter coastal polynyas may be quickly swept away along the coast. In contrast, there is a relatively quiet nearshore region to the west, between Cape Lisburne and Icy Cape, where dense water may accumulate much longer and continue to become denser before it is carried across the shelf. *INDEX TERMS:* 4207 Oceanography: General: Arctic and Antarctic oceanography; 4255 Oceanography: General: Numerical modeling; 4532 Oceanography: Physical: General circulation; 4536 Oceanography: Physical: Hydrography; *KEYWORDS:* Arctic Ocean, Pacific Water, Chukchi Sea

Citation: Winsor, P., and D. C. Chapman (2004), Pathways of Pacific water across the Chukchi Sea: A numerical model study, *J. Geophys. Res.*, *109*, C03002, doi:10.1029/2003JC001962.

1. Introduction

[2] The Chukchi Sea acts as a conduit for water flowing into the Arctic Ocean from the North Pacific Ocean and the Bering Sea (Figure 1), where it has a prominent effect on the thermohaline and biogeochemical structure of the Arctic Ocean. Pacific Water is generally fresher and warmer (during summer) than its counterpart in the Arctic Ocean, and can be traced in the Canadian Basin by its characteristic warmer temperature, evident in vertical profiles at about 50 m depth. Pathways within the Arctic Basin are not fully understood, but Pacific Water can be traced across the Arctic Ocean to the northern tip of Greenland [*Jones et al.*, 1998]. During winter, the Pacific Water is modified during it transit across the broad Chukchi shelf and eventually contributes to the cold halocline layer of the Arctic Basin [*Swift et al.*, 1997]. The Pacific Water throughflow also plays an important role in the global freshwater budget [e.g., *Wijffels et al.*, 1992].

[3] Bering Strait provides the only path for exchange of water, ice, heat and nutrients between the Pacific and Arctic

0148-0227/04/2003JC001962$09.00

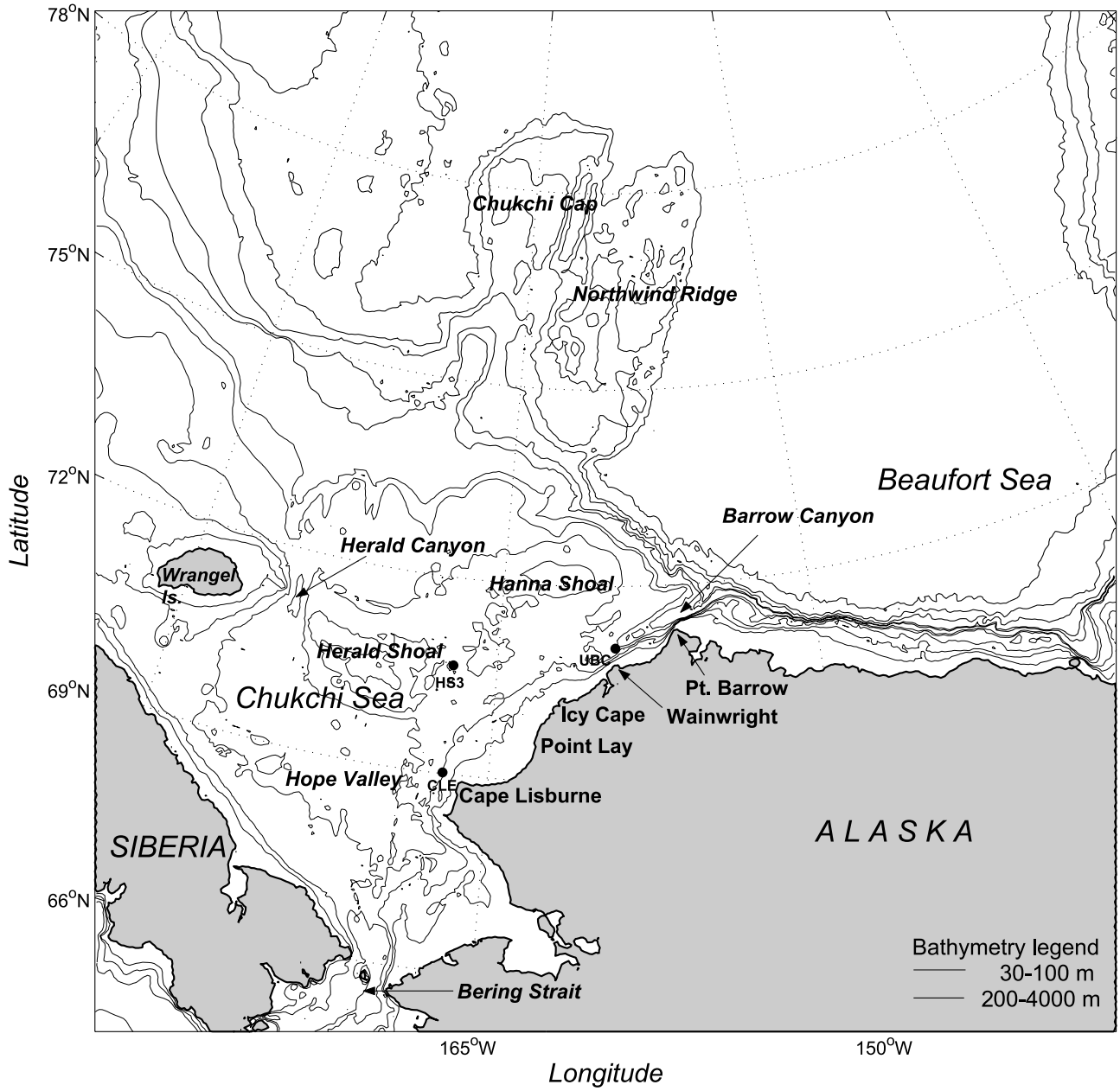

Figure 1. Bathymetry and mooring locations in the Chukchi and Beaufort Seas. Bathymetric data are from the International Bathymetric Chart of the Arctic Ocean (IBCAO) database. Isobaths are drawn for 30, 40, 50, 75, 100, 200, 250, 500, 1000, 2000, and 4000 m. Isobaths are thin for 30–100 m, and thick for 200–4000 m depth.

Oceans. The mean flow is northward, driven by a mean salinity difference between the fresher North Pacific Ocean and the saltier Arctic Ocean, which gives rise to a steric height difference of ~0.5 m, translating to a sea level slope of $\sim 10^{-6}$ [*Stigebrandt*, 1987]. The annual mean transport is believed to be in the 0.6–0.9 Sv range [*Coachman and Aagaard*, 1966, 1981; *Aagaard et al.*, 1985]. More recent observations from both Doppler and mechanical current measurements over a four-year period suggest that the mean transport is 0.8 ± 0.1 Sv [*Roach et al.*, 1995]. Short-term flows can be much smaller or larger in response to local wind events, including complete reversals [*Aagaard et al.*, 1985; *Johnson*, 1989]. The Bering Strait inflow is generally smaller during winter due to more frequent northerly winds, and larger in summer with overall weaker winds.

[4] Once the Pacific Water has passed Bering Strait, it flows into the broad and shallow Chukchi Sea. The circulation and pathways that the flow takes across the Chukchi Sea are not fully understood. Hydrographic and current measurements suggest that the flow separates into three branches [e.g., *Coachman et al.*, 1975]. The best documented branch roughly follows the Alaskan coastline, through the Chukchi Sea and into the Beaufort Sea, and is called the Alaska Coastal Current [*Coachman et al.*, 1975]. The mean transport of this current is uncertain, but it is estimated to carry ~0.3 Sv (T. Weingartner, personal

communication, 2003). This current is also subject to short-term reversals during times of strong winds from the northeast and east [*Weingartner et al.*, 1998]. The second branch is believed to flow northwest through Hope Valley, following the topography into Herald Canyon, while the third and weakest branch is found between Herald and Hanna Shoals (T. Weingartner, personal communication, 2003). The transports and ultimate fate of the latter two branches are highly uncertain. For example, Pacific Water is found north of the Chukchi shelf edge, over the Chukchi Cap, Northwind Ridge and Canada Abyssal Plain [*Jones et al.*, 1998], but it is unclear if this water originates from the inflow directly, or if it has been recirculated from the Beaufort Sea by the general anti-cyclonic circulation found offshore there.

[5] The circulation of Pacific Water and the specific pathways followed are of great importance to the biogeochemical conditions, including interaction with bottom sediments and biota. The different pathways that these waters may take can alter the nutrient content and, therefore, the potential for strong primary production across the Chukchi shelf [*Grebmeier*, 1993]. In a larger perspective, winter-time water mass modification occurring on the broad, shallow shelf determines whether the nutrient-rich waters end up in the mixed-layer, cold halocline layer or if they are sequestered in the deep ocean.

[6] Some previous studies attempted to model the Bering Strait throughflow using barotropic models. For example, *Proshutinsky* [1986] simulated the Bering Strait inflow and circulation on the Chukchi shelf by imposing a sea level slope across Bering Strait and found that the flow bifurcated into two branches, one directed toward the northwest and one along the Alaskan coast. *Overland and Roach* [1987] imposed a sea level difference between the Pacific and Arctic Oceans to force a northward flow through Bering Strait, and found that a 0.4 m sea level difference resulted in a 0.6 Sv transport. Using a similar approach, *Spaulding et al.* [1987] found a 1.97 Sv northward transport induced by a 10^{-6} sea surface slope. The latter two studies were aimed at understanding the driving of the Bering Strait throughflow rather than the specific pathways of flow across the Chukchi shelf, and none of these studies examined the fate of the throughflow upon reaching the shelf edge. Furthermore, they each used rather coarse model resolution, so they could not elucidate the details of the transport pathways. Several Pan-Arctic models also exist, but they tend not to consider the detailed circulation of the Chukchi Sea and the Bering Strait inflow explicitly.

[7] We present here results from a high-resolution, two-dimensional barotropic model, aimed at understanding the circulation pathways of Pacific Water across the Chukchi Sea and the effect of wind-forcing on these pathways. We recognize that a barotropic model has many limitations, especially in regions of deep water and/or stratification. However, most of the Chukchi Sea is quite shallow (<50 m) and weakly stratified, so a barotropic model is adequate to obtain a first-order understanding of the circulation there. We present our model setup in section 2, followed by a suite of results in section 3, including the sensitivity to wind-forcing. Then, in section 4, we compare our results with observations, estimate dynamic response times and advective travel times, examine some statistics of local winds that are important to trace reversals in the coastal flow, and suggest some implications for dense shelf water formation. Our conclusions follow in section 5.

2. Model Description

[8] The model used here is the Regional Ocean Model System (ROMS), a free-surface, hydrostatic, primitive equation ocean model that uses stretched, terrain-following coordinates in the vertical and orthogonal curvilinear coordinates in the horizontal. ROMS solves the standard Boussinesq momentum, temperature, salinity and continuity equations. Details can be found on the ROMS website (http://marine.rutgers.edu/po/index.php?model=roms). For the present study, we configured ROMS in a two-dimensional barotropic mode with linearized bottom stress with a coefficient set to a typical value of $r = 5 \times 10^{-4}$ m s^{-1}, and uniform rotation with Coriolis parameter $f = 1.4 \times 10^{-4}$ s^{-1}. The sensitivity of the results to the bottom friction coefficient is discussed in section 4. No additional smoothing or lateral mixing is applied in the model.

[9] The model domain covers the entire Chukchi shelf, extends well northwest of Wrangel Island into the East Siberian Sea (to about 165°E), stretches eastward along the entire Beaufort shelf, and extends northward beyond the shelf edge, including the Northwind Ridge and Chukchi Cap to ~78°N (Figure 2). The size of the domain is 2100 × 1500 km. The model domain has open boundaries on the north, south, and west edges, at which a Flather radiation condition is applied [*Flather*, 1976]. Bathymetry is taken from the International Bathymetry Chart of the Arctic Ocean (IBCAO) with a spatial resolution of 2.5 km [*Jakobsson et al.*, 2000]. The bathymetry is interpolated to match our uniform 4 km grid, with no maximum cut off in depth. The coastline is placed along the 15 m isobath.

[10] We first run the model without wind forcing, starting from rest, with an unperturbed sea-surface height over the whole model domain. The inflow through Bering Strait is prescribed at the southern model boundary as a steady, northward flow of 0.8 Sv distributed evenly across Bering Strait. Using a time step of 10 s, the model is run for 20 days, by which time the flow has essentially reached steady state everywhere in the model domain. (In fact, steady state is achieved over the shelf within about 10 days.) This steady state, which we call the no-wind case, is then used as the initial condition for the wind-driven calculations, in which a uniform, steady wind stress is applied in a specified direction over the whole domain. The wind stress is typically applied for 10 days. All other energy sources, such as atmosphere-ocean fluxes or ice stresses, are ignored.

[11] All calculations use the entire domain shown in Figure 2. However, virtually all of the circulation generated by the Bering Strait inflow is limited to the inner box drawn around the Chukchi Sea, so only results from this region are presented below. Figure 2 also shows the locations of six sections at which transport computations are made below.

[12] We expect the flows in such a shallow sea to be strongly affected by the bottom topography, so it is useful to point out a few of the prominent features apparent in Figure 1. Hope Valley is broad and relatively deep (~50 m), extending north-northwest from Bering Strait, where it

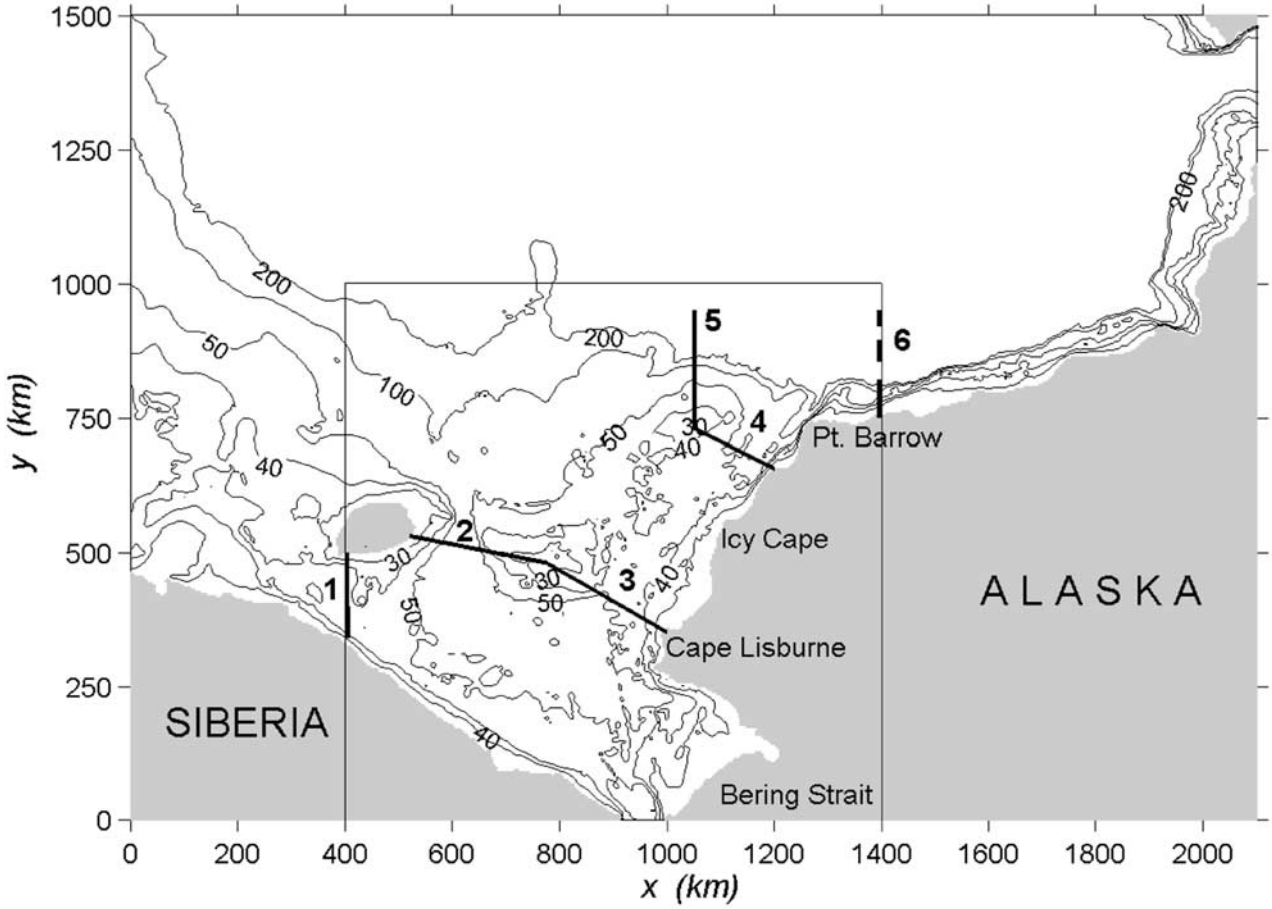

Figure 2. Map of the model domain, including detailed bathymetry and locations of sections 1 to 6 used for transport computations. Isobaths are contoured at 30, 40, 50, 100 and 200 m. Section 1 is from Wrangel Island to the Siberian coast, section 2 is from Herald Shoal to Wrangel Island, section 3 is from Herald Shoal to Cape Lisburne, section 4 is from the Alaskan coast to Hanna Shoal, section 5 is from Hanna Shoal across the shelfbreak to the 300 m isobath, and section 6 is from Cape Halkett across the Beaufort shelf to the 300 m isobath (solid line) and 150 km farther offshore (dashed line). The inner box shows the part of the domain within which results are presented.

eventually narrows to form Herald Canyon, located between Wrangel Island and Herald Shoal. Following the Alaskan coast northeast from Bering Strait is a relatively broad channel, which narrows as it approaches Barrow Canyon. Farther out on the shelf, there is a deeper channel between Herald and Hanna Shoals, with maximum depth of ~50 m, commonly known as the Central Channel. To the east of Barrow Canyon is the relatively narrow Beaufort shelf, where it is about 100 km from the coast to the 100 m isobath, beyond which the bathymetry is very steep down to ~3000 m.

3. Results

3.1. Large-Scale Circulation: Bering Strait Inflow Only

[13] Here we explore the steady state barotropic currents driven only by an imposed steady northward flow of 0.8 Sv through Bering Strait, i.e., the no-wind case. Figure 3 shows depth-averaged current vectors after 20 days within the region of the inner box in Figure 2, along with streamlines computed from the velocity field ($uh = -\psi_y$, $vh = \psi_x$ where u, v are horizontal velocities in the coordinates of Figure 2, h is depth, ψ is stream function and subscripts x, y denote partial differentiation). Several interesting features are visible. The circulation of Pacific waters across the Chukchi shelf forms a broad flow with local areas of intensified currents, and all inflowing water eventually ends up flowing past Pt. Barrow and moving eastward along the narrow Beaufort shelf. In more detail, the Bering Strait inflow immediately forms a strong current that is steered toward the northwest by a depression in the local bathymetry, and then broadens as it enters Hope Valley. Some of the flow continues northwestward, becomes intensified as it encounters Herald Canyon, and then turns eastward. The remainder of the flow turns north-northeast, moving to the east of Herald Shoal. Some of this flow winds its way between Herald and Hanna Shoals, where it is moderately intensified before again turning eastward toward the Alaskan coast. Virtually all of the throughflow eventually joins together between Icy Cape and Pt. Barrow to form the most intense

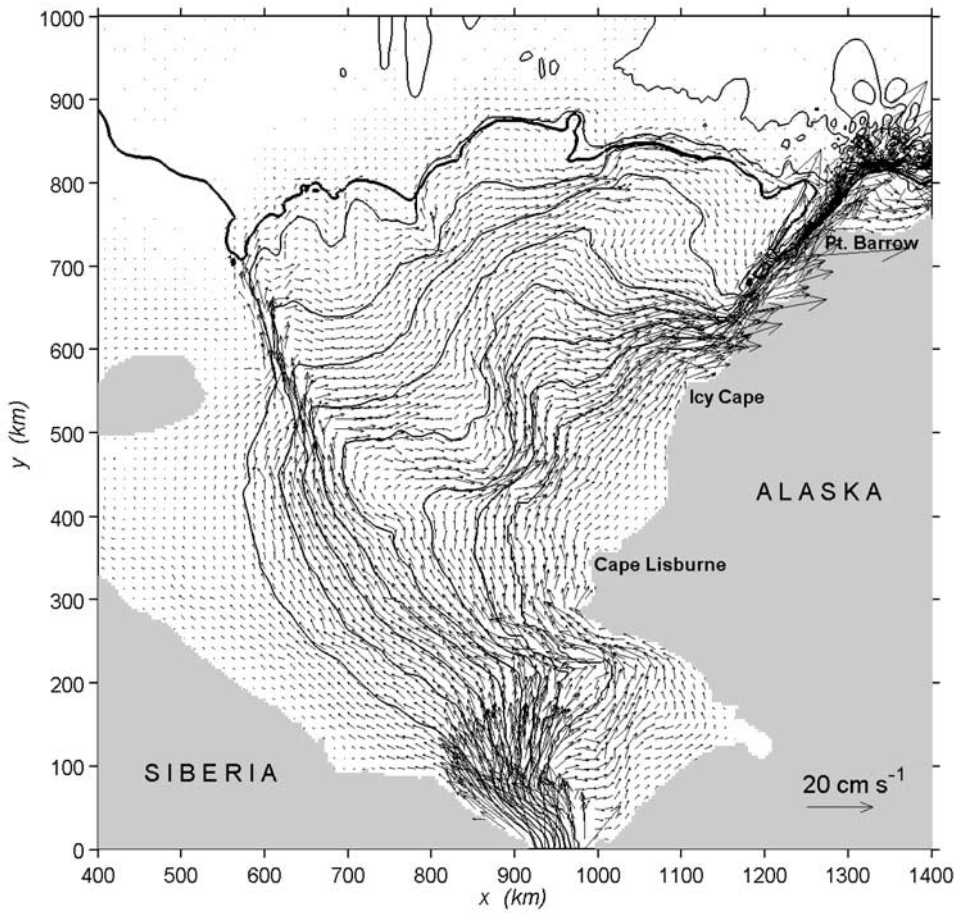

Figure 3. Streamlines with barotropic current vectors overlaid for the no-wind case. Streamline contours are 0.1 Sv, and current vectors are plotted every third grid point. Also shown is the 100-m isobath (solid thick line).

current, which squeezes between the coast and Barrow Canyon before moving onto the Beaufort shelf. Such an intensified flow near Pt. Barrow has been observed in several studies [e.g., *Münchow and Carmack*, 1997; *Weingartner et al.*, 1998]. Once past Pt. Barrow, the intensified current separates from the coast as it flows onto the Beaufort shelf, forming a shelfbreak jet located at ~100 m depth. This is consistent with a recent analysis of historical hydrographical measurements as described by *Pickart* [2004]. Note that the coastal currents are much weaker between Cape Lisburne and Icy Cape than from Icy Cape to Pt. Barrow, a point to which we will return in section 4.

[14] Figure 3 clearly shows three areas of locally intensified currents over the central Chukchi shelf, consistent with the three branches described in the Introduction; Herald Canyon, between Herald and Hanna Shoals (the Central Channel), and along the Alaskan coast between Icy Cape and Pt. Barrow. However, the streamlines in Figure 3 also show that the intensified currents are not strictly separate branches but are actually part of a single broad current system. For example, a portion of the intensified flow in Herald Canyon escapes the canyon, turning eastward to join the current in the Central Channel. Part of this current then turns eastward to join the coastal current. Ultimately, the water in the coastal jet between Icy Cape and Pt. Barrow contains water that has passed through both Herald Canyon and the Central Channel. Thus the three regions of intensified currents are not independent, and the sum of their transports will not generally equal the total inflow through Bering Strait.

[15] Once the inflow moves north of Cape Lisburne, about 50% (~0.4 Sv) of it flows northwest through Hope Valley, and an equal amount flows northeast along the Alaskan coast toward Barrow Canyon. Transports through sections 1 to 6, denoted in Figure 2, help to quantify these flow features. (Positive transport signifies flow toward the north and/or east.) The transport in section 1, between Wrangel Island and the Siberian coast, is very small (−0.03 Sv) and is directed toward the northwest. The transport between Wrangel Island and Herald Shoal (section 2) is large (0.39 Sv), including most of the northward flow that enters Herald Canyon. The remaining inflow transport (0.40 Sv) passes between Herald Shoal and Cape Lisburne (section 3). Further to the northeast, the transports between the coast and Hanna Shoal (section 4), and between Hanna Shoal and the shelfbreak (section 5) are 0.52 and 0.18 Sv, respectively. Thus the transport between the coast and Hanna Shoal (section 4) represents 65% of the total inflow through Bering Strait, owing to the confluence of waters mentioned above. The transport across the western

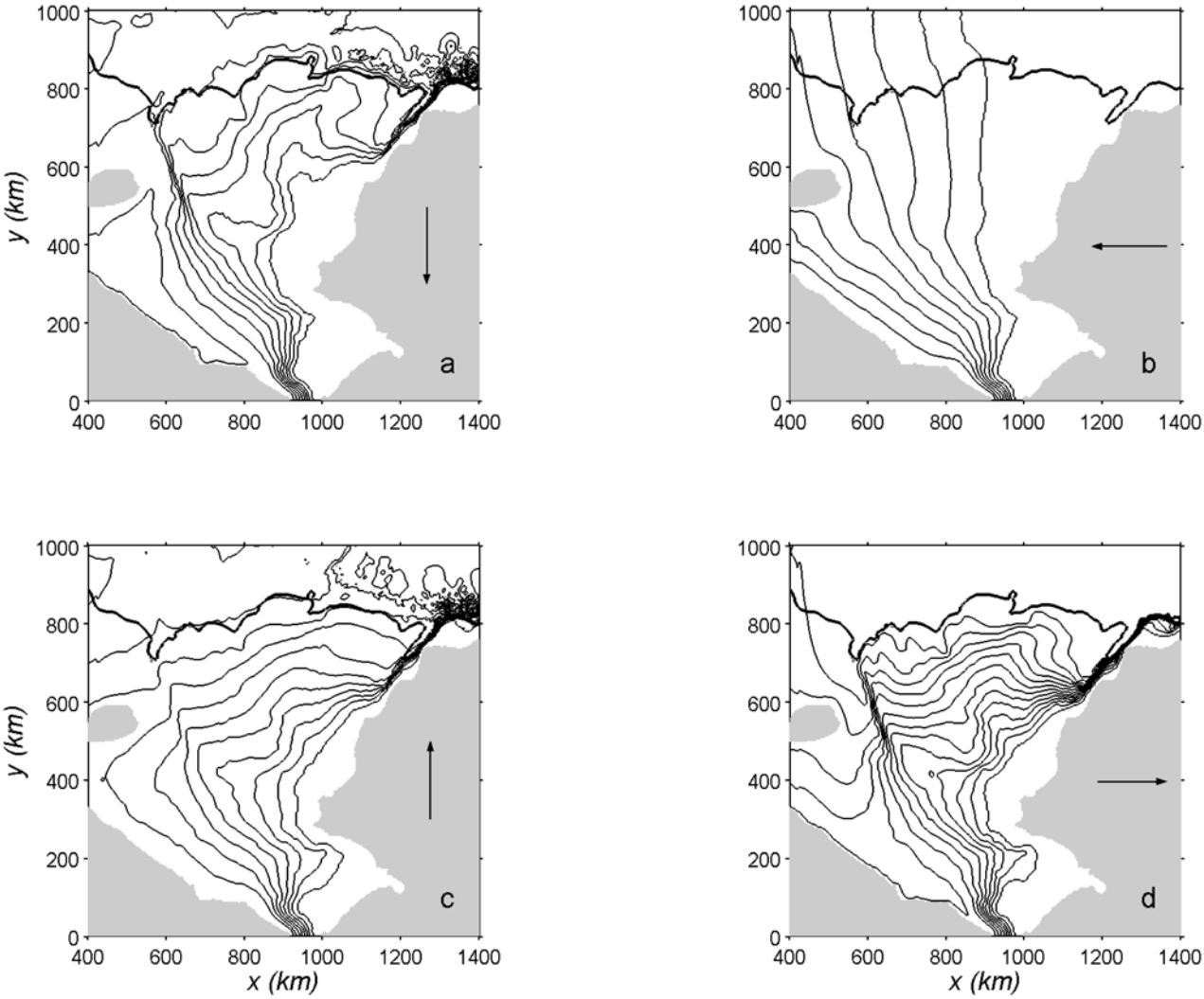

Figure 4. Streamlines after a 10-day steady wind stress of 0.1 Pa ($\sim$7.7 m s^{-1}) from (a) north, (b) east, (c) south, and (d) west. Streamline contours are 0.1 Sv. Also shown is the 100-m isobath (thick solid line). Arrows indicate wind direction.

end of the Beaufort shelf to the 300 m isobath (section 6) is eastward with 0.62 Sv. If section 6 is extended 150 km farther offshore (dashed line in Figure 2), nearly all of the imposed inflow through Bering Strait can be accounted for (0.78 Sv or 0.98%). Thus for this no-wind case, there is virtually no transport of Pacific Water across the shelf edge into the interior Canada Basin.

3.2. Idealized Wind-Forcing

[16] Wind forcing can substantially alter the shelf circulation in the Chukchi Sea [e.g., *Aagaard et al.*, 1985; *Johnson*, 1989; *Weingartner et al.*, 1998]. To investigate the first-order effect of winds on the circulation described above, we have conducted a number of idealized model runs. Each calculation starts from the steady state flow field of the no-wind case (Figure 3). We then apply a uniform, constant wind stress of 0.1 Pa ($\sim$7.7 m s^{-1}) over the entire model domain for 10 days. The wind direction is varied from 0°T to 315°T in 45°T increments.

[17] The overall response of the circulation to changing wind directions (winds from the north, east, south, and west) is shown in Figure 4, expressed in terms of streamlines (contoured every 0.1 Sv). Northerly winds (Figure 4a) produce only minor changes in the circulation, including a weak southward flow along the Siberian coast between Wrangel Island and Siberia, and a small recirculation between Icy Cape and Cape Lisburne along the Alaskan coast (not obvious here because of the contour interval). Easterly winds (Figure 4b) change the circulation fundamentally, producing nearly parallel streamlines aligned northward. The flow ignores prominent bathymetrical features, and Pacific Water flows into the interior Canada Basin. Even the flow along the Alaskan coast separates at Cape Lisburne and moves northward from there. The coastal jet at Pt. Barrow is now reversed, though much weaker, flowing toward Bering Strait (not shown here, but see Figure 12b). About 0.27 Sv of Pacific Water flows northwest between Wrangel Island and the Siberian coast toward the East Siberian Sea, while the remaining transport of $\sim$0.5 Sv flows northward off the shelf and into deeper waters. Southerly winds (Figure 4c) have little effect on the large-scale circulation, basically producing a more evenly

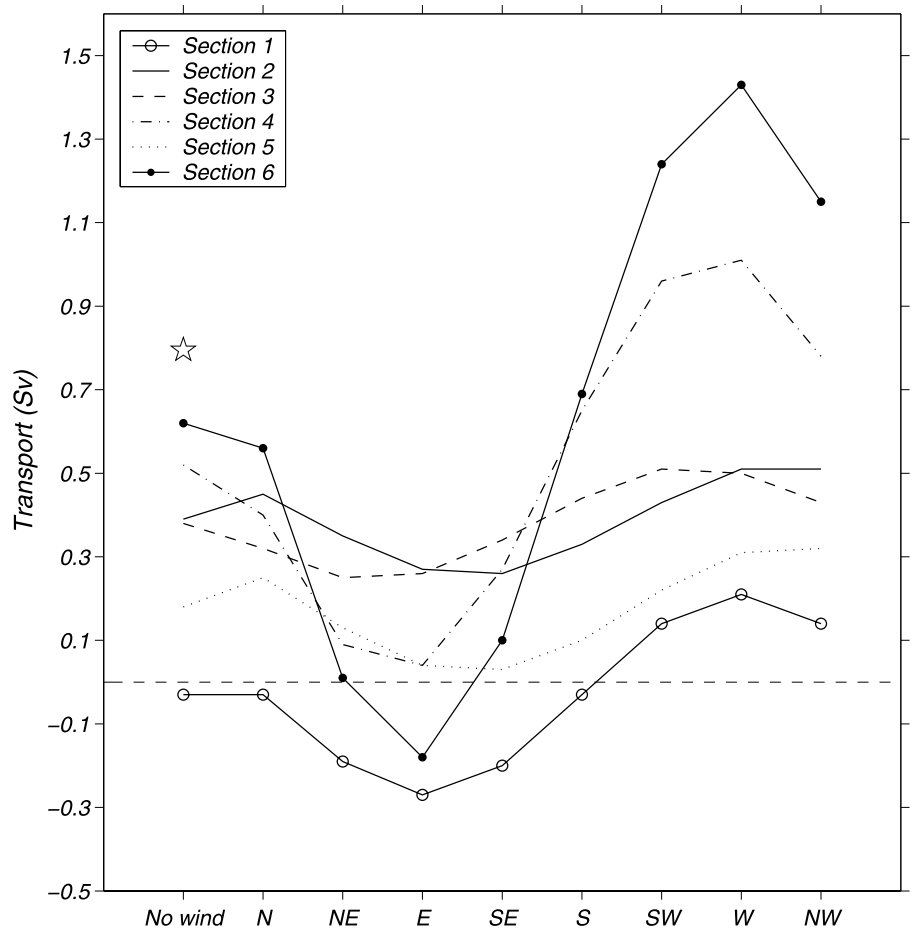

Figure 5. Transport in sections 1 to 6 for different wind directions. A constant wind stress of 0.1 Pa ($\sim$7.7 m s^{-1}) was applied for each direction for a 10-day period starting from the steady state flow field of the no-wind run. The no-wind run transports are also shown, where the star represents the transport through section 6 if extended 150 km farther offshore to include part of the deeper waters (dashed line in Figure 2).

distributed flow over the shelf. Westerly winds (Figure 4d) produce overall intensified currents and a very strong coastal jet past Pt. Barrow, with maximum current speed of 83 cm s^{-1}. Additional transport comes from the northwest because the westerly wind stress sets up a sea level pressure gradient along the Siberian and Alaskan coasts.

[18] The effect of wind forcing on the transports through sections 1–6 (Figure 2) is presented in Figure 5 for each different wind direction. The results from the no-wind case are also shown. There are two basic patterns of the circulation. One resembles the no-wind case or an intensified version of the no-wind case, with larger transports at each section but overall flow in the same direction as the no-wind case. This pattern occurs for winds from the north, northwest, west, southwest, south and to some extent southeast (e.g., Figures 4a, 4c, and 4d). Virtually all of the transport exits the Chukchi Sea around Pt. Barrow and then enters the Beaufort shelf. Transports through sections 4 and 6 may be large in these cases. The second pattern occurs for winds from the northeast or east (e.g., Figure 4b). There is a strong reduction in transport through all sections, to the point where the transports through sections 4 and 5 nearly vanish, while the transport through section 6 reverses completely to carry −0.18 Sv westward ($\sim$22% of the Bering Strait inflow). Interestingly, section 3 (Herald Shoal to Cape Lisburne) is rather insensitive to changing wind directions, appearing about the same in both flow patterns, with a northeasterly transport averaging $\sim$0.4 Sv (50% of the inflow).

[19] Several additional calculations have been made to determine how strong the wind stress must be to reverse the flow on the Beaufort shelf and along the Alaskan coast. An easterly wind stress is imposed for 10 days with magnitude varying from 0 to 0.1 Pa (0 to $\sim$7.7 m s^{-1}), in increments of 0.0125 Pa. For weak winds (Figure 6a), the primary effect is to reverse the nearshore currents on the Beaufort shelf to flow westward. The jet along the Alaskan coast is not significantly altered from the no-wind case, but once on the Beaufort shelf, it flows to the east as a narrow current concentrated at the shelf edge (along the 100 m isobath). A wind stress of 0.075 Pa ($\sim$6.6 m s^{-1}) is required to produce a major change in the nearshore circulation along the Alaskan coast (Figure 6b). Now the Beaufort shelf-edge flow is effectively stopped, and a strong westerly flow is present, extending from the shore nearly to the shelf edge and as far west as Barrow Canyon. Here it meets a much-reduced and broadened Alaskan Coastal Current, still directed toward the northeast, but

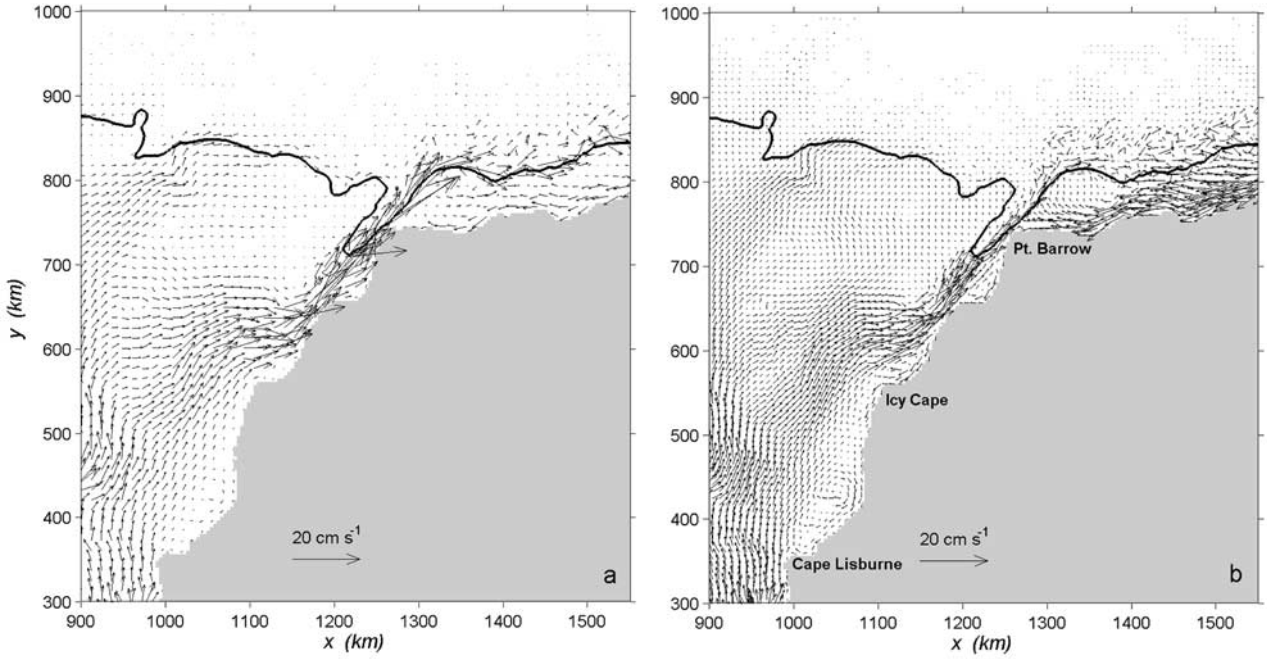

Figure 6. Detailed plots of barotropic current vectors along the Alaskan coast and Beaufort shelf for different values of easterly wind stress, (a) 0.05 Pa ($\sim$5.4 m s^{-1}) and (b) 0.075 Pa ($\sim$6.6 m s^{-1}). Vectors are plotted every second grid point. Also shown is the 100-m isobath (solid thick line).

now separated from the coast by a weak flow reversal extending from Pt. Barrow to Cape Lisburne. Stronger winds further strengthen the reversed coastal current and weaken the northeastward offshore flow. These results suggest that a wind stress exceeding $\sim$0.07 Pa ($\sim$6.4 m s^{-1}) can reverse the flow near Pt. Barrow.

[20] The distribution of the barotropic currents across the Beaufort shelf (section 6) and between Wrangel Island and Herald Shoal (section 2) is shown in Figure 7 for different directions of wind forcing. In the no-wind case (thick solid lines), there is eastward flow in section 6 toward the Beaufort Sea (positive velocities in Figure 7a), with highest velocities concentrated in a jet $\sim$45–50 km offshore, at about the 100 m isobath. The shelf flow is $\sim$40 km wide, while the jet width is $\sim$15 km. Winds from the west tend to increase the eastward currents, with the jet positioned at the same offshore location but with velocities reaching 50 cm s^{-1}. Winds from the north or south give similar cross-shelf properties as the no-wind case. Winds from the east reverse the flow (as noted above) but also change the cross-shelf structure, with the highest velocities now occurring close to the coast and then gradually decreasing offshore. This is caused by the wind-driven sea level setup, which is largest at the coast. The velocities across section 2, between Wrangel Island and Herald Shoal, are quite different (Figure 7b). Here virtually all transport occurs within Herald Canyon with the highest velocities concentrated on the eastern side in a 20 km wide core (positive is northward). The transport is toward the north-northeast for all wind directions except winds from the east, for which the transport is greatly reduced.

[21] The response of the shelf circulation to wind-forcing described above can be understood to a large extent simply by superimposing the effects of the Bering Strait inflow and the wind-forcing. The inflow introduces a sea level setup and subsequent pressure gradient along the Alaskan coast and the Beaufort shelf, driving the northeasterly flow. Winds transport water to their right, which produces setup or setdown along the coastlines. Westerly winds produce sea level setup that adds to that generated by the Bering Strait inflow, thereby increasing the alongshore pressure gradient and resulting in an intensified circulation. The opposite occurs for easterly winds, where the setup from the inflow is reduced by the wind setdown, resulting in a net sea level decrease along the Siberian coast and along the Beaufort shelf with the consequent northward flow into the deep basin (Figure 4b).

3.3. Dynamic Response Time

[22] So far we have investigated the steady state circulation produced by a constant inflow through Bering Strait (the no-wind case) and the changes caused by a uniform, steady wind stress. It is also of interest to know how quickly the circulation responds to wind events. We anticipate a response time based on the spindown timescale for barotropic flow, h/r, where h is the depth and r is the bottom friction coefficient. For a typical shelf depth of 50 m and $r = 5 \times 10^{-4}$ m s^{-1}, the spindown timescale is $h/r \approx 1.2$ days. This is an e-folding timescale, so we expect a new steady state to be fully established after 2 or 3 e-folding times, or roughly 2–3 days. Of course, the response time will be longer in deeper water, e.g., offshore of the shelf edge. To demonstrate, we examine the response of the no-wind case to suddenly imposed easterly winds, and then the response as the flow relaxes when the wind-forcing is abruptly halted.

[23] Figure 8a shows the time evolution of the transports through sections 4 to 6 for an easterly wind stress with a total duration of 10 days. Sections 4 and 5 respond quickly, reaching a new steady state within about 2 days, as expected

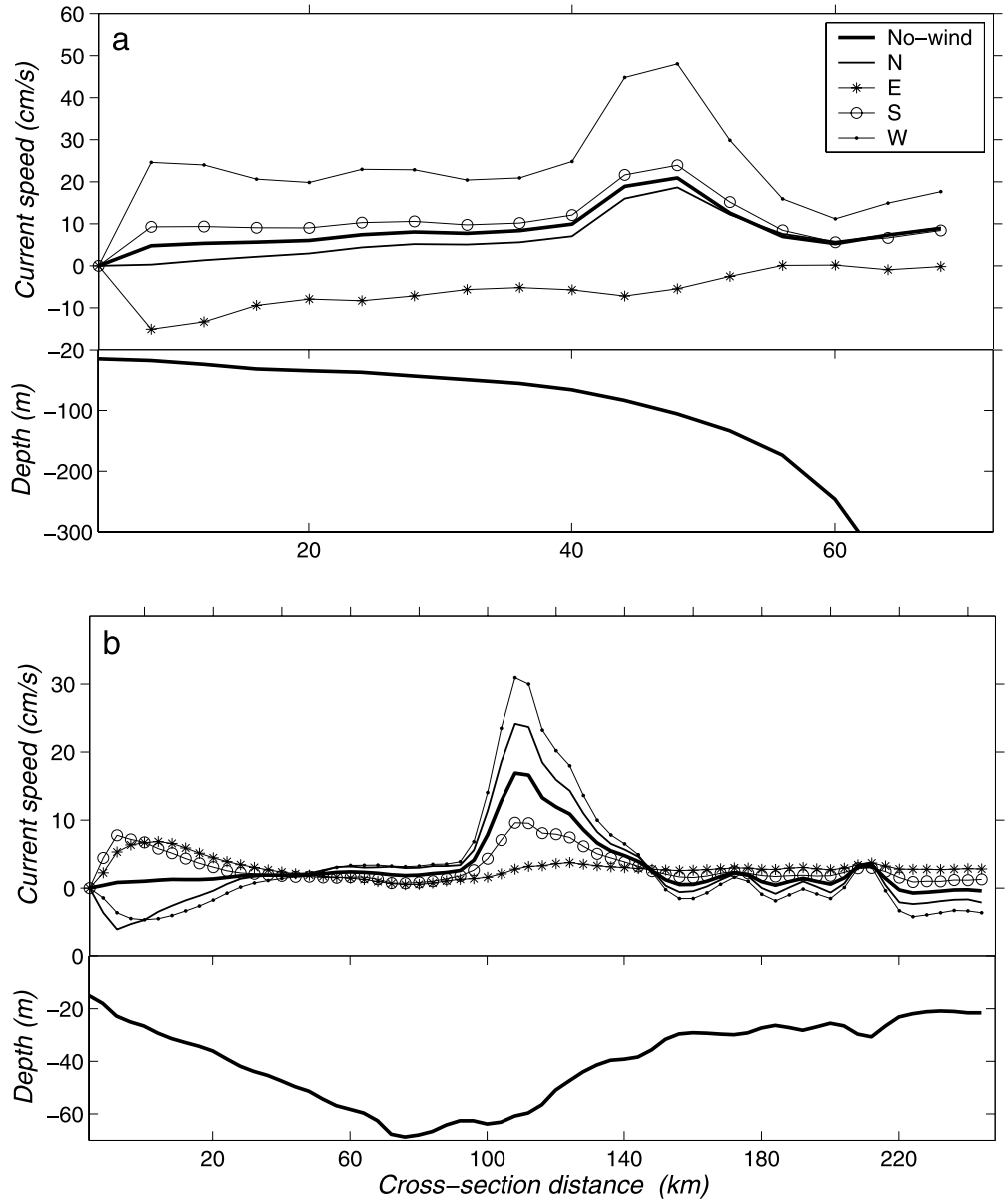

Figure 7. Cross-section barotropic current velocities for different wind directions together with corresponding cross-section bathymetry at (a) section 6 (the Beaufort shelf), and (b) section 2 (Wrangel Island to Herald Shoal). Positive currents are eastward in Figure 7a and northward in Figure 7b.

for the shelf flow. In the easternmost section (section 6), the current has reversed completely after ~2 days and remains reversed with only a slight change with time between days 4 and 10. The time to reach the new steady state is about 3 days, slightly longer than the other sections because section 6 includes some deeper water. Figure 8b shows the transports through the same sections, but now turning off the wind stress after 3 days. Until day 3, everything is identical to the case shown in Figure 8a. After day 3, the circulation responds within about 2–3 days to restore the original no-wind circulation. Thus h/r provides a good estimate of the dynamic response time for this system.

3.4. Advection Time

[24] The streamlines presented in Figures 3 and 4 clearly illustrate that water flowing in from the western or eastern sides of Bering Strait will circulate around different parts of the Chukchi Sea, experiencing a variety of current strengths and directions along their paths. Furthermore, the circulation patterns change rapidly (within a few days) in response to altered forcing. That is, the dynamical information propagates through the region quickly. However, these results do not indicate how long it takes for a water parcel to travel from Bering Strait to any point along its individual streamline. This advection time (or travel time) is an indication of how rapidly water properties are carried across the Chukchi Sea and the amount of time available for mixing and exchange with surrounding water masses. We have computed advection times along each streamline by integrating the reciprocal of the velocity along the streamline. The resulting advection times are shown in Figure 9 along three different streamlines in three cases; the no-wind

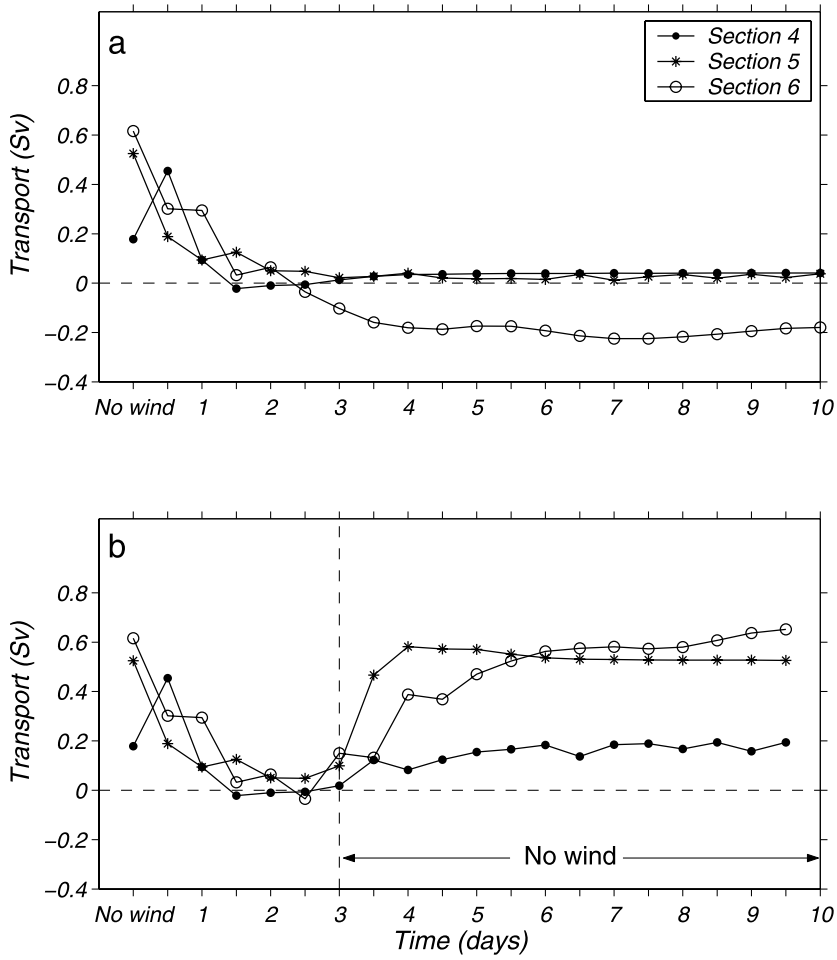

Figure 8. Time evolution of transport in sections 4 to 6 for (a) a constant 10-day steady easterly wind stress of 0.1 Pa ($\sim$7.7 m s^{-1}), and (b) a 3-day constant easterly wind stress of 0.1 Pa ($\sim$7.7 m s^{-1}) followed by no wind stress for a 7-day period. The no-wind transports are also shown.

case and winds from the east and west. Advection times are expressed in months, with each dot in Figure 9 representing one month of travel time from the inflow at Bering Strait and a few selected dots showing the number of months for easy reference.

[25] The no-wind case (Figure 9a) shows that water from the western part of Bering Strait, flowing northwest through Herald Canyon, takes $\sim$1 year to cross the Chukchi shelf, and another 1.5 years to flow along the shelf edge before reaching Pt. Barrow, in all $\sim$2.5 years (30 months). In contrast, water entering the Chukchi Sea through the eastern part of Bering Strait needs only $\sim$5–6 months to reach the same destination. This difference in travel time ($\sim$2 years) is surprisingly large.

[26] Winds greatly alter the advection times. For easterly winds (Figure 9b), the northwestward flow along the Siberian coast is fast, taking $\sim$4 months to reach Wrangel Island. The interior northward flow directly across the Chukchi shelf is initially rapid, taking 6 months to cross about 3/4 of the distance between Bering Strait and the shelf edge, but then slowing down considerably as the water depth increases. It takes about one year for water to reach the shelf edge in this case. For westerly winds (Figure 9c), the flow resembles that of the no-wind case, but now with much shorter travel times for the western inflow. Water following the westernmost streamline entering through Bering Strait now turns eastward much sooner and only takes $\sim$7 months to reach Pt. Barrow, compared to 30 months in the no-wind case.

[27] As mentioned above, the advection times estimated here are important for water masses to exchange both physical and biogeochemical properties with surrounding waters. The 2.5-year advection time found for the westerly inflow through Bering Strait in the no-wind case is particularly interesting because this water is believed to be relatively salty and nutrient rich, compared to its eastern counterpart. The long advection time suggests that this water mass may reside on the Chukchi shelf long enough to undergo two seasonal cycles and probably contribute to primary production before exiting the shelf.

4. Discussion

4.1. Comparison With Observations

[28] Here we compare currents from the no-wind case with those observed from moored instruments presented by *Weingartner et al.* [1998] and from ship-borne ADCPs (T. J. Weingartner et al., manuscript in preparation, 2003), fully recognizing that a comparison between flows in a steady state barotropic model and observations at discrete locations

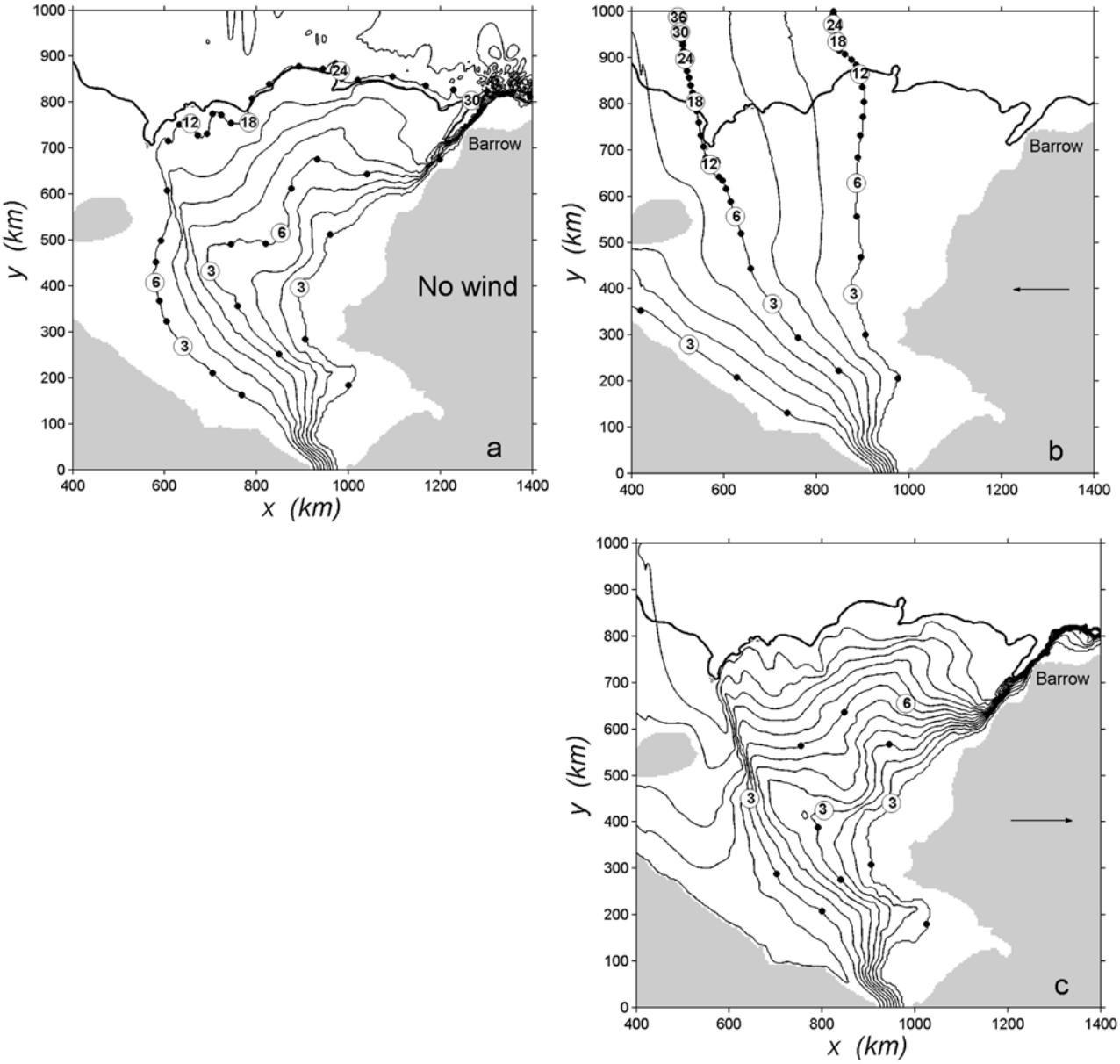

Figure 9. Streamlines (as in Figure 4) together with advection time along three selected streamlines for (a) no-wind case, (b) easterly winds, and (c) westerly winds, with a wind stress of 0.1 Pa ($\sim$7.7 m s^{-1}). Each dot represents one month of advection time from the inflow at Bering Strait, with a few selected dots showing the number of months for easy reference (see text for details).

and/or times may be problematic. Our goal is merely to investigate to what extent the main features seen in the modeled circulation are present in observations. First, we compare currents at three moorings located on the northeast Chukchi shelf (CLE, HS3, and UBC in Figure 1). The results are summarized in Table 1. Mooring HS was located east of Herald Shoal, just where the current intensifies in our no-wind case. *Weingartner et al.* [1998] observed a mean current velocity of 8.2 cm s^{-1} directed toward 350°T, at 50 m depth, 3 m from the bottom. The direction suggests bathymetric steering, in concert with our model estimate. The model produces a velocity of 6.2 cm s^{-1} at this location, with almost the same direction as the observations (355°T). Mooring CLE was located offshore of Cape Lisburne, at roughly the 40 m isobath. *Weingartner et al.* [1998] found weak currents at CLE of 3.0 cm s^{-1} with a direction of 345°T, very close to the model current of $\sim$3 cm s^{-1} with direction 353°T. Mooring UBC was located at the head of Barrow Canyon within the model coastal jet, and the observed mean velocity was quite strong at 20 cm s^{-1} directed toward 60°T. The model current at this location is remarkably similar, with velocity 22 cm s^{-1} directed toward 65°T. Overall, the depth-averaged model currents compare quite well with the long-term mean currents reported by *Weingartner et al.* [1998], especially considering the simplicity of the model and its forcing.

[29] *Weingartner et al.* [1998] also found that the currents at Barrow Canyon were coherent with those at Herald Shoal

Table 1. Statistics of Current Meters and Modeled Barotropic Currents[a]

Mooring	Position		Speed, cm s^{-1}	Direction, °T	Model Speed, cm s^{-1}	Model Direction, °T
	Lat (°N)	Long (°W)				
UBC	71°3′	159°3′	20.2	60	22.0	65
HS3	70°40′	167°2′	8.2	350	6.3	355
CLE	69°1′	166°57′	3.0	345	3.3	350

[a]Mooring data as described in *Weingartner et al.* [1998, Tables 1a and 2]. Model speeds and directions are taken from the nearest grid points encompassing the mooring positions.

on timescales larger than ~3 days. This is consistent with our finding of a broad circulation with a response time of 2–3 days. During strong northeasterly winds, observed currents at UBC were reversed toward the southwest, while they remained northeastward but weak at CLE. The modeled circulation during northeasterly or easterly winds matches this well, with a reversed nearshore current, while maintaining a northeastward flow off Cape Lisburne (see Figure 6).

[30] Figure 10 shows vertically averaged current vectors from ship-borne, underway ADCP measurements in the Chukchi Sea from 22 to 25 September 1993 and from 16 September 1995 (T. J. Weingartner et al., manuscript in preparation, 2003). The raw data were originally averaged over 4 m in the vertical, and written every 2 min. Analyzing the current velocities at different depths, we found that they were fairly similar, indicating mainly barotropic flow. The ADCP measurements show several features that coincide with our model no-wind case. First, there is an intensified northward flow in Herald Canyon, similar to the model results (Figure 7b), with high current velocities concentrated on the eastern part of the canyon. Second, ADCP currents between Herald and Hanna Shoals show slightly higher current speeds at the eastern flank of Herald Shoal, directed toward the northeast, while the flow in the eastern part of the section is slower and directed toward the southeast. This is consistent with our modeled scenario; a confluence of water flowing northeast along the east flank of Herald Shoal, with some water recirculating near Hanna Shoal toward the southeast, joined there by water that has traveled through Herald Canyon and along the shelf edge (Figure 3). Third, there is a strong coastal jet past Pt. Barrow, coincident with the highest current velocities in our model at this location. *Münchow and Carmack* [1997] also present evidence of this

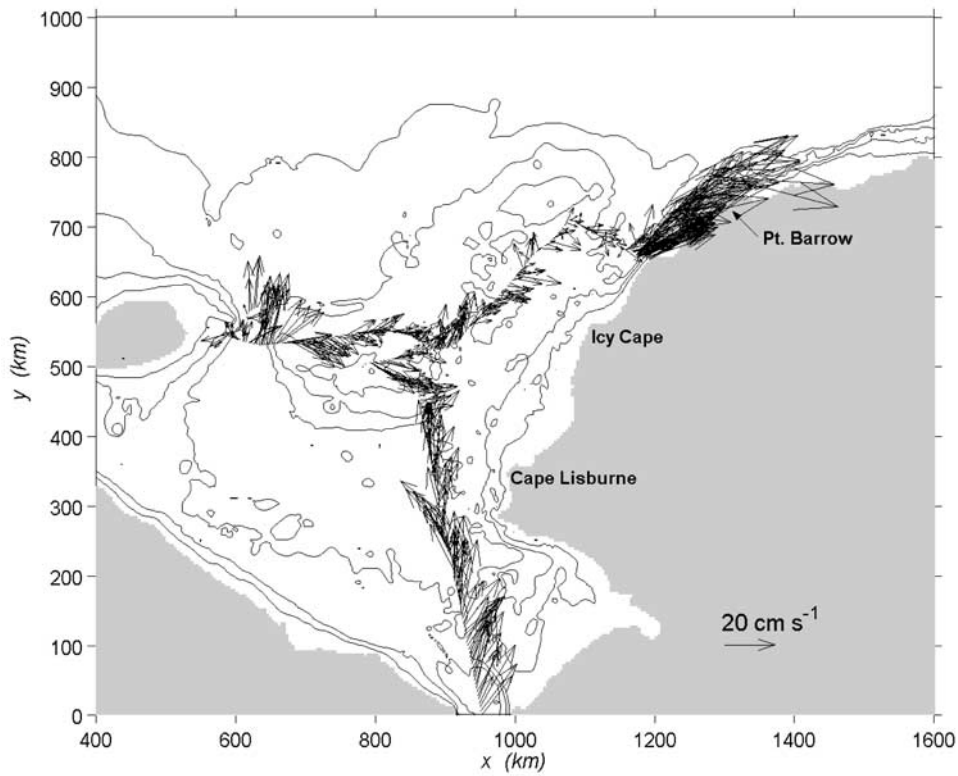

Figure 10. Vertically averaged current vectors from 300 kHz narrow-band ADCP data, collected in the Chukchi Sea between 22 and 25 September 1993 (northeasterly transect from Bering Strait to Barrow) and 16 October 1995 (Wrangel Island to Herald Canyon transect). The raw data were originally averaged 4 m in the vertical, and 2 min in time. Also shown are the 30, 40, 50 and 100 m isobaths. ADCP data courtesy of Tom Weingartner and Seth Danielson, University of Alaska, Fairbanks.

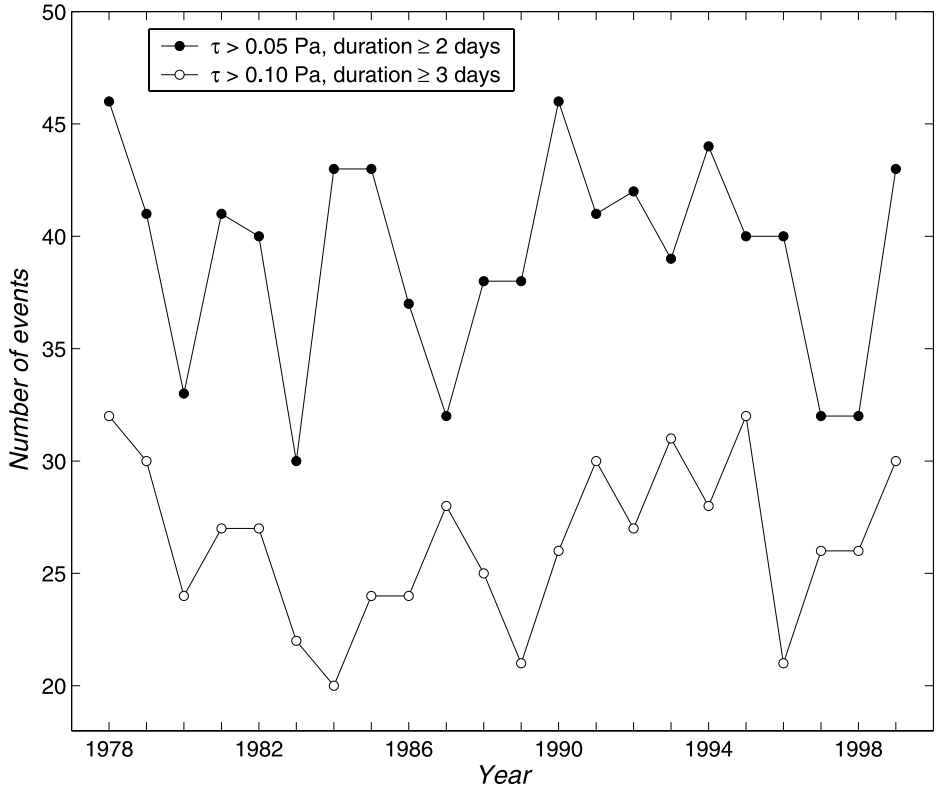

Figure 11. Wind statistics derived from 6-hourly meteorological observations at Barrow (WMO station 70026) for the 1978 to 1999 period, showing number of events per year with winds between 35–100°T for wind stress exceeding 0.05 Pa (~5.4 m s^{-1}) with a duration of ≥2 days (filled circles), and for wind stress exceeding 0.1 Pa (~7.7 m s^{-1}) with a duration of ≥3 days (open circles).

jet using ADCP measurements. Other ADCP measurements from 1995 (not shown) show a much weaker, partly reversed coastal flow, when northeasterly winds prevailed, similar to the modeled coastal current during northeasterly to easterly winds, and much like the regional wind event described by *Johnson* [1989].

4.2. Wind Statistics

[31] The modeled circulation is sensitive to northeasterly to easterly winds, resulting in reversed nearshore flow along the Alaskan coast and generally northward flow over most of the Chukchi shelf. It is important to gain some knowledge of the frequency with which such winds may occur. Here we use land-based meteorological station data to investigate the statistics of wind events that might produce large changes in the standard circulation. We have compared wind records from three stations; Barrow (WMO number 70026), Wainwright (WMO number 70030), and Pt. Lay (WMO number 70121), see Figure 1 for locations. These stations were chosen because they are located near the coast, away from interfering topography, and have long-term homogenous observations. These stations may not represent the wind field over the entire model domain, and may also suffer from local effects such as sea breeze [see e.g., *Kozo*, 1979]. However, we feel that they give valuable insight into prevailing winds along the Alaskan coast and Beaufort shelf. Statistics were compiled for the 1978 to 1999 period using 6-hourly observations. We found that the wind speed and direction at the three stations are quite coherent over the 22-year period investigated, so we present here only the results from Barrow, which has the best temporal coverage of the three stations.

[32] Statistics of wind events from 35 to 100°T were computed. For each continuous event lasting longer than 1 day, we made statistics of the duration, wind speed, and direction. The mean duration is ~3 days, with only a few events lasting more than 10 days. The 3-day duration is consistent with the timescale of low-pressure systems in the Arctic, and coincides with the typical response time of our model. This may help to explain the frequent and short-term reversals seen in the mooring data of *Weingartner et al.* [1998]. Longer events (>5 days) are not uncommon, representing ~17% of all events longer than 1 day. Such events should be able to produce a well-defined reversed coastal current, and advect some Pacific Water into the central Canada Basin.

[33] We also investigated the interannual variability of wind events from 35 to 100°T, for two different cases; events with a minimum duration of 2 days and with a wind stress >0.05 Pa (~5.4 m s^{-1}), and events with a 3-day minimum duration, with a wind stress > 0.1 Pa (~7.7 m s^{-1}, Figure 11). The first case represents events with a moderate impact on the circulation, only partly reversing the circulation on the Beaufort Shelf, while the coastal jet at Pt. Barrow is still northeastward but weaker. The second case includes events strong enough to reverse the nearshore circulation completely, including the Pt. Barrow jet. The mean number of events per year with winds from this sector

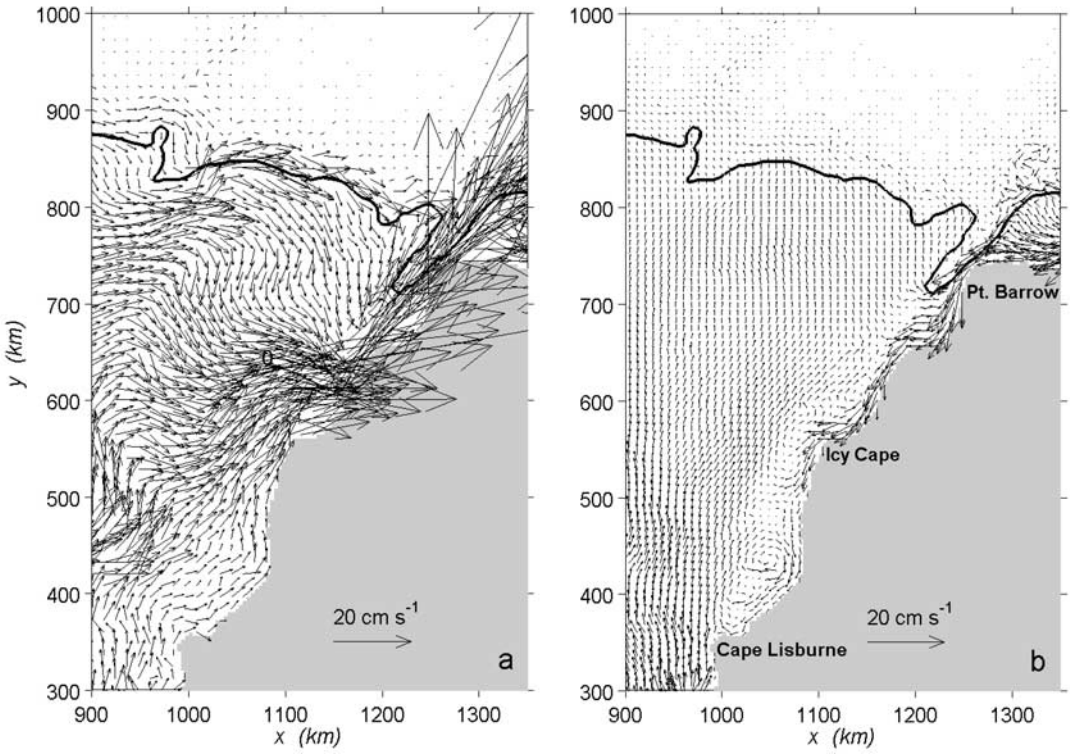

Figure 12. Detailed plots of barotropic current vectors along the Alaskan coast where frequent polynyas form during winter, for (a) steady westerly winds and (b) steady easterly winds. Vectors are plotted every third grid point in Figure 12a, and every second grid point in Figure 12b. Also shown is the 100-m isobath (solid thick line).

is 39 and 26 for the two cases, respectively, rather evenly distributed throughout the year. Strong reversals can thus be expected fairly regularly, with some years having as many as 30 well-defined reversals.

4.3. Implications for Dense Shelf Water Formation

[34] The area between Cape Lisburne and Pt. Barrow has been identified in several studies as an active site for polynya formation and dense water production [e.g., *Cavalieri and Martin*, 1994; *Winsor and Björk*, 2000]. The offshore transport of dense shelf water produced here may be controlled by baroclinic instabilities, causing small-scale eddies to form that can carry the dense water across isobaths to deeper waters [*Gawarkiewicz and Chapman*, 1995; *Chapman*, 2000; *Winsor and Chapman*, 2002]. This mechanism is, however, limited by strong alongshelf currents [*Chapman*, 2000; *Signorini and Cavalieri*, 2002], and is thus favored in areas with weak currents and active polynyas.

[35] The model results show that the distribution of currents along the Alaskan coast is sensitive to the wind direction and strength. During easterly winds (Figure 12b), nearshore currents are reversed and offshore currents are much weaker and broader than either the westerly wind case (Figure 12a) or the no-wind case (Figure 3). In terms of dense water formation, this circulation favors the accumulation of salty water and perhaps the formation of hypersaline waters that may ventilate the cold halocline layer or even penetrate to deeper lying layers. This is basically the scenario suggested by *Weingartner et al.* [1998]; i.e., easterly winds tend both to open polynyas and to stop or reverse the Alaska Coastal Current, allowing hypersaline water to form, which is swept toward Barrow Canyon when the winds relax and the coastal current is reestablished. The mean easterly winds over the Chukchi Sea and the increased wind variance during winter further enhance both polynya activity and dense water formation.

4.4. Model Sensitivity and Simplifications

[36] Our modeling philosophy is to keep things simple, while still learning something fundamental about the pathways of Pacific Water across the Chukchi shelf. Hence we considered a fairly simple barotropic model with idealized forcing, while resolving bathymetric features. In reality, there are many more factors that could potentially affect the results presented here. These include ambient density stratification, a seasonally buoyant inflow through Bering Strait, ice cover, freshwater inflows from rivers, the large-scale remotely forced circulation in the deep basin, spatial variations in the winds, to name some. Nevertheless, the general agreement between the model and the limited observations is encouraging. The observed flow seems to be fairly barotropic, steered by bathymetry and sensitive to wind-forcing, all of which are captured reasonably well in our model. One problematic area is the narrow Beaufort shelf and slope between Pt. Barrow and the Mackenzie River outlet to the east. The bathymetry is very steep here, and we do not resolve this properly with 4 km resolution. In fact, resolution of less than 0.5 km is probably needed here. Other effects not considered are the combined effect of

wind-forcing and changes in the Bering Strait inflow, i.e., we change the wind-forcing but keep the inflow constant. However, the two forcings are not dynamically independent, so future modeling should address this issue. We have made some additional model runs to test the linearity of the model response. In particular, we repeated the no-wind calculation, but with the nonlinear terms omitted, and found the resulting circulation to be remarkably similar to the fully nonlinear no-wind case. We also ran the no-wind case with different constant values of the Bering Strait inflow, and the system behaved linearly, i.e., halving the inflow halves the transports on the shelf.

[37] The wind stress we use could be viewed as either ice-ocean stress or direct wind stress on the water. Ice does not usually move in exactly the same direction as the surface wind, even during free drift, so this would change the direction and magnitude of the stress felt by the ocean. Similarly, during mid winter, the ice cover on the Chukchi shelf can be less movable due to internal ice stresses, which could limit or severely reduce the stress applied to the underlying ocean. These effects should be investigated in future studies.

[38] Finally, we use linear bottom friction with a coefficient of 5×10^{-4} m s^{-1} throughout this paper. Given the linear nature of the response, bottom friction is the primary force causing cross-isobath motions in the no-wind case, producing the flow in Figure 3. That is, without bottom friction, this steady linear flow would follow isobaths exactly. To investigate the sensitivity of our results to this choice, we conducted a number of additional model runs of the no-wind case, varying the coefficient between 2.5 and 7.5×10^{-4} m s^{-1}. The transport in sections 1 to 6 changed very little (less than 5%). Individual current vectors changed, especially in the low-friction case, but the overall circulation is rather insensitive to this choice. Finally, we ran the no-wind case using quadratic bottom friction with a coefficient of 2.5×10^{-3}. Individual current vectors differed slightly, but the overall circulation is unchanged, with prominent features such as the coastal jet at Barrow Canyon being quite similar. Overall transports in sections 1 to 6 are nearly identical, with a maximum difference in transport of 0.06 Sv.

5. Conclusions

[39] Pathways of Pacific Water flowing from the North Pacific Ocean through Bering Strait and across the Chukchi Sea have been investigated using a two-dimensional barotropic model. We have considered flow driven by a prescribed steady northward flow of 0.8 Sv through Bering Strait and modified by idealized wind-forcing. We have found that

[40] 1. The Bering Strait throughflow alone (no-wind case) produces a steady state circulation consisting of a broad northeasterly flow, basically following the topography, with a few areas of intensified currents. About half of the inflow travels northwest through Hope Valley, while the other half turns somewhat toward the northeast along the Alaskan coast. The flow through Hope Valley is intensified as it passes through Herald Canyon, but much of this flow escapes the canyon to move eastward, joining the flow in the broad valley between Herald and Hanna Shoals (Central Channel), another area of slightly intensified currents. Thus the flow does not separate into truly distinct branches.

[41] 2. In the no-wind case, there is a confluence of nearly all of the flow along the Alaskan coast west of Pt. Barrow to create a very strong and narrow coastal jet that follows the shelf topography eastward onto the Beaufort shelf. Thus in this case, nearly all of the Pacific Water entering the Chukchi Sea eventually ends up flowing eastward along the narrow Beaufort shelf, with no discernable flow across the shelf edge toward the interior Canada Basin.

[42] 3. The no-wind case flow field is relatively insensitive to uniform wind-forcing when the winds are from the south, west or north, in which cases the shelf transports tend to be intensified. However, northeasterly to easterly winds are able to completely reverse the flows along the Beaufort shelf and the Alaskan coast. Such winds also force most of the throughflow in a more northerly direction across the Chukchi shelf edge, potentially supplying the surface waters of the interior Canada Basin with Pacific Water.

[43] 4. The entire shelf circulation reacts promptly to changing wind conditions, with a dynamic response time of $\sim$2–3 days. However, travel times for water parcels to move from Bering Strait to Pt. Barrow vary tremendously according to the path taken: less than 6 months along the Alaskan coast, and about 30 months along the westernmost path through Herald Canyon. Wind forcing from the west greatly reduces the travel time of particles entering on the western side of Bering Strait.

[44] 5. The model results support the scenario for dense shelf water formation suggested by *Weingartner et al.* [1998]. That is, easterly winds, which tend to open coastal polynyas, also stop or reverse the Alaska Coastal Current, allowing hypersaline water to form. This dense water is then swept toward Barrow Canyon when the winds relax and the coastal current is reestablished.

[45] The results presented here elucidate some aspects of the circulation in the Chukchi Sea, and they are reasonably consistent with observations. However, there is much room for future work, including the effects of stratification and a buoyant inflow of fresher Pacific water. Another important and interesting question is the modification of Pacific water on the Chukchi shelf as it is cooled and interacts with the seasonal ice cover. Further improvement in our understanding will, of course, require detailed observational efforts, and we hope that idealized process modeling efforts like that presented here might help guide mooring placements and hydrographic measurements.

[46] **Acknowledgments.** We thank Tom Weingartner and Seth Danielson for generously sharing unpublished ADCP data, and Roger Goldsmith for his assistance with extraction of bathymetric data and model grid construction. We also thank Knut Aagaard, Glen Gawarkiewizc, Bob Pickart, Andrey Proshutinsky, Tom Weingartner, and Rebecca Woodgate for many valuable comments on our paper. Financial support was provided to PW by the Postdoctoral Scholar Program at the Woods Hole Oceanographic Institution (WHOI), the Swedish Foundation for International Cooperation in Research and Higher Education (STINT), and the J. Seward Johnson Fund. Funding for DCC came through a grant from the Coastal Ocean Institute at WHOI. We are grateful for this support. Woods Hole Oceanographic Institution contribution 10930.

References

Aagaard, K., A. T. Roach, and J. D. Schumacher (1985), On the wind-driven variability of the flow through Bering Strait, *J. Geophys. Res.*, *90*, 7213–7221.

Cavalieri, D. J., and S. Martin (1994), The contribution of Alaskan, Siberian, and Canadian coastal polynyas to the cold halocline layer of the Arctic Ocean, *J. Geophys. Res.*, *99*, 18,343–18,362.

Chapman, D. C. (2000), The influence of an alongshore current on the formation and offshore transport of dense water from a coastal polynya, *J. Geophys. Res.*, *105*, 24,007–24,019.

Coachman, L. K., and K. Aagaard (1966), On the water exchange through Bering Strait, *Limnol. Oceanogr.*, *11*, 44–59.

Coachman, L. K., and K. Aagaard (1981), Re-evaluation of water transports in the vicinity of Bering Strait, in *The Eastern Bering Sea Shelf: Oceanography and Resources*, vol. 1, edited by D. W. Hood and J. A. Calder, pp. 95–110, Natl. Oceanic Atmos. Admin., Washington, D. C.

Coachman, L. K., K. Aagaard, and R. B. Tripp (1975), *Bering Strait: The Regional Physical Oceanography*, 172 pp., Univ. of Washington Press, Seattle.

Flather, R. A. (1976), A tidal model of the north-west European continental shelf, *Mem. Soc. R. Sci. Liege*, *10*, 141–164.

Gawarkiewicz, G., and D. C. Chapman (1995), A numerical study of dense water formation and transport on a shallow, sloping continental shelf, *J. Geophys. Res.*, *100*, 4489–4507.

Grebmeier, J. M. (1993), Studies of pelagic benthic coupling extended onto the Soviet continental shelf in the Northern Bering and Chukchi Seas, *Cont. Shelf Res.*, *13*, 653–668.

Jakobsson, M., N. Z. Cherkis, J. Woodward, R. Macnab, and B. Coakley (2000), New grid of Arctic bathymetry aids scientists and mapmakers, *Eos Trans. AGU*, *81*, 89.

Johnson, W. R. (1989), Current response to wind in the Chukchi Sea: A regional coastal upwelling event, *J. Geophys. Res.*, *94*, 2057–2064.

Jones, E. P., L. G. Anderson, and J. H. Swift (1998), Distribution of Atlantic and Pacific waters in the upper Arctic Ocean: Implications for circulation, *Geophys. Res. Lett.*, *25*, 765–768.

Jones, E. P., J. H. Swift, L. G. Anderson, M. Lipizer, G. Civitarese, K. K. Falkner, G. Kattner, and F. McLaughlin (2003), Tracing Pacific water in the North Atlantic Ocean, *J. Geophys. Res.*, *108*(C4), 3116, doi:10.1029/2001JC001141.

Kozo, T. L. (1979), Evidence for sea breezes on the Alaskan Beaufort Sea coast, *Geophys. Res. Lett.*, *6*, 849–852.

Münchow, A., and E. C. Carmack (1997), Synoptic flow and density observations near an Arctic shelf break, *J. Phys. Oceanogr.*, *27*, 1402–1419.

Overland, J. E., and A. T. Roach (1987), Northward flow in the Bering and Chukchi Seas, *J. Geophys. Res.*, *92*, 7097–7105.

Pickart, R. S. (2004), Shelf break circulation in the Alaskan Beaufort Sea: Mean structure and variability, *J. Geophys. Res.*, doi:10.1029/2003JC001912, in press.

Proshutinsky, A. (1986), Calculating surge fluctuations in the level and circulation of water of the Chukchi Sea, *Meteorol. Gidrologia*, *1*, 54–61.

Roach, A. T., K. Aagaard, C. H. Pease, S. A. Salo, T. Weingartner, V. Pavlov, and M. Kulakov (1995), Direct measurements of transport and water properties through Bering Strait, *J. Geophys. Res.*, *100*, 18,443–18,457.

Signorini, S. R., and D. J. Cavalieri (2002), Modeling dense water production and salt transport from Alaskan coastal polynyas, *J. Geophys. Res.*, *107*(C9), 3136, doi:10.1029/2000JC000491.

Spaulding, M., T. Isaji, D. Mendelsohn, and A. C. Turner (1987), Numerical simulation of wind-driven flow through Bering Strait, *J. Phys. Oceanogr.*, *17*, 1799–1816.

Stigebrandt, A. (1987), The North Pacific: A global-scale estuary, *J. Phys. Oceanogr.*, *14*, 464–470.

Swift, J. H., E. P. Jones, K. Aagaard, E. C. Carmack, M. Hingston, R. W. MacDonald, F. A. McLaughlin, and R. G. Perkin (1997), Waters of the Makarov and Canada basins, *Deep Sea Res., Part II*, *44*, 1503–1529.

Weingartner, T. J., D. J. Cavalieri, K. Aagaard, and Y. Sasaki (1998), Circulation, dense water formation, and outflow on the northeast Chukchi shelf, *J. Geophys. Res.*, *103*, 7647–7661.

Wijffels, S. E., R. W. Schmitt, H. L. Bryden, and A. Stigebrandt (1992), Transport of freshwater by the oceans, *J. Phys. Oceanogr.*, *22*, 155–162.

Winsor, P., and G. Björk (2000), Polynya activity in the Arctic Ocean from 1958 to 1997, *J. Geophys. Res.*, *105*, 8789–8803.

Winsor, P., and D. C. Chapman (2002), Distribution and interannual variability of dense water production from coastal polynyas on the Chukchi shelf, *J. Geophys. Res.*, *107*(C7), 3079, doi:10.1029/2001JC000984.

D. C. Chapman and P. Winsor, Physical Oceanography Department, Woods Hole Oceanographic Institution, Woods Hole, MA 02543, USA. (pwinsor@whoi.edu)